

# Spectral observations of Seyfert galaxies with the spectrograph UAGS at the Rozhen NAO\*

Boyko Mihov, Lyuba Slavcheva-Mihova, Georgi Petrov  
Institute of Astronomy, Bulgarian Academy of Sciences,  
72 Tsarigradsko Chausse Blvd., Sofia 1784, Bulgaria  
bmihov@astro.bas.bg  
(Conference talk)

**Abstract.** We present the results of the spectral observations of the Seyfert galaxies Mrk 335, Mrk 509 and NGC 7469 (NGC 7469 being the main target) obtained with UAGS at Rozhen NAO. These observations are a part of a programme aiming to adapt a CCD camera as a detector of UAGS. Our results show that UAGS equipped with a CCD camera could become a useful constituent of the spectral apparatus at Rozhen NAO.

**Key words:** Galaxies: individual: Mrk 335, Mrk 509, NGC 7469 – Galaxies: Seyfert – techniques: spectroscopic

## Спектрални наблюдения на Сифърт галактики със спектрографа UAGS на НАО Рожен

Бойко Михов, Люба Славчева-Михова, Георги Петров

Представяме резултатите от спектралните наблюдения на Сифърт галактиките Mrk 335, Mrk 509 и NGC 7469 (NGC 7469 беше нашата главна цел), получени със спектрографа UAGS на НАО Рожен. Наблюденията са част от програма по адаптиране на CCD камера като приемник на спектрографа UAGS. Нашите резултати показват, че спектрографът UAGS, оборудван със CCD приемник, може да се превърне в полезна част от спектралната апаратура, с която разполага НАО Рожен.

## Introduction

Spectral observations with the 2.0-m telescope of the Rozhen National Astronomical Observatory of Bulgaria (NAO) could be performed using the following equipment: Coudé spectrograph for high resolution spectroscopy of bright objects, Universal Astronomical Grating Spectrograph (UAGS) for medium resolution spectroscopy and single/two-channel Focal Reducer Rozhen (FoReRo/FoReRo-2) with grism for low resolution spectroscopy. We shall not consider furthermore the Coudé spectrograph as it is not applicable for our aims – spectroscopy of Active Galactic Nuclei (AGNs).

Spectral observations of AGNs at NAO during the period 1983 – 1990 were performed using UAGS, manufactured by Carl Zeiss Jena, and a two/three-stage image-intensifying tube with electrostatic focusing; the spectra were registered on a photographic film. An example of a spectrum taken with UAGS during this period is shown in Fig. 1, where the spectrum of the galaxy Ark 144 nucleus is plotted. Some results of the spectral study of the Seyfert galaxies Mrk 1040, MCG +8–11–11 and NGC 7469 based on UAGS spectra taken at NAO were presented by Slavcheva et al. [1998]. These spectra were taken using UAGS and the three-stage image-intensifying tube with electrostatic focusing XX1063; their inverse linear dispersion (simply dispersion hereafter) is 50 Å/mm. For a short period of time around 1983 the registration of spectra could be done by means of a cooled vidicon functioning in combination with the Optical Multichannel Analyser OMA-1205 (Tsvetkov & Markov [1984]). However, this apparatus was used occasionally; in particular, no AGN spectra were obtained with it.

At the beginning of the nineties of the 20-th century the spectral observations of AGNs with UAGS were left off. The spectroscopy of AGNs was resumed at the beginning of the 21-th century when the previously built focal reducer FoReRo was employed

---

\* Based on observations obtained at the Rozhen National Astronomical Observatory of Bulgaria operated by the Institute of Astronomy, Bulgarian Academy of Sciences.

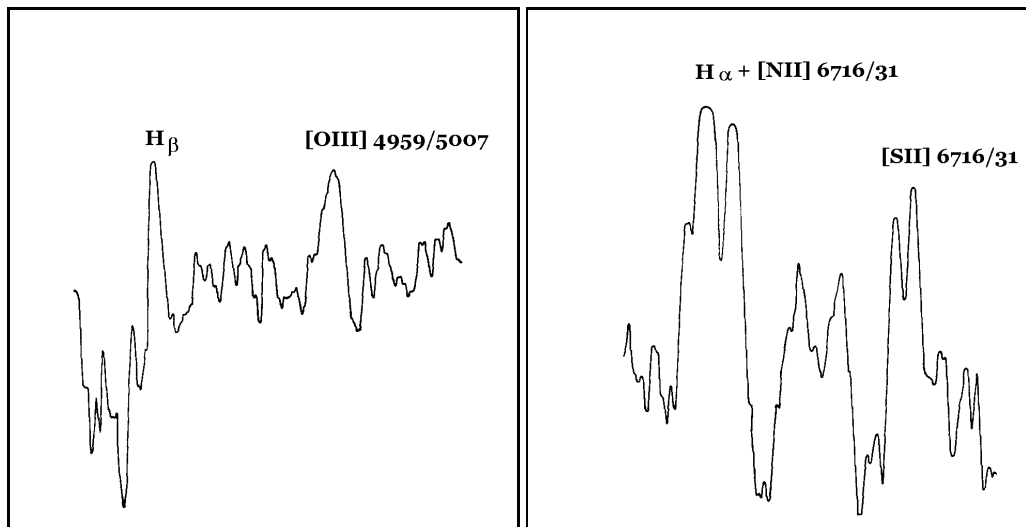


**Fig. 1.** Density tracing of the spectrum of the galaxy Ark 144 nucleus. Abscissa is in units of Angstroms and the wavelength increases to the right. This 50 Å/mm dispersion spectrum have been taken using UAGS and the three-stage image-intensifying tube with electrostatic focusing XX1063.

to perform low resolution spectroscopy of bright AGNs – the first test spectra were obtained by G. Petrov and L. Slavcheva-Mihova in May 2002, and the first results of bright quasar spectroscopy were published by Semkov et al. [2005]. However, some problems, for example, the accurate decomposition of complex emission line profiles, demand higher resolution. And this higher resolution could be provided by the forgotten UAGS. By reason of this, adaptation of a CCD camera as a detector of UAGS was initiated<sup>1</sup>; note that UAGS was designed to be used with photographic plates as detectors and, therefore, the usage of a CCD detector is not straightforward.

In this paper we present the first spectra of good quality obtained using UAGS equipped with a CCD camera as a detector. The main target of our spectroscopy was NGC 7469 – a well studied Seyfert 1.2 type galaxy at  $z = 0.016317$ . According to our July 1998 measurements the galaxy  $V$  band flux is 13 mag in a 10 arcsec diameter aperture.

## 1 Observations and data reduction

The observations were performed during the night of August 31/September 1, 2003 under good atmospheric conditions – a clear sky, 1–1.5 arcsec seeing. UAGS was attached to the Ritchey-Chrétien focus of the 2.0-m telescope; a 651 grooves/mm grating<sup>2</sup> that gives 100 Å/mm dispersion in the first order was used. The two-stage Peletier cooled SBIG ST-6 model CCD camera was used as a detector; ST-6 has  $375 \times 242$  pixels area,  $23 \times 27 \mu\text{m}$  pixel size and a conversion factor of 6.7 e/ADU. The CCD camera was attached to the external focal plane of the UAGS 150 mm Schmidt camera and was oriented so that the narrower pixel size should be along the dispersion. The spectrum obtained with this configuration covers a spectral interval of 861 Å and has a dispersion

<sup>1</sup> The first usage of a CCD camera as a detector of UAGS was made by E. Semkov in March 1993. He used SBIG ST-6 CCD camera to register the spectrum of the long-term variable star RT Cep. However, no more observations were made.

<sup>2</sup> Gratings having 325 and 1302 grooves/mm are also available; they give dispersions of 200 and 50 Å/mm, respectively.

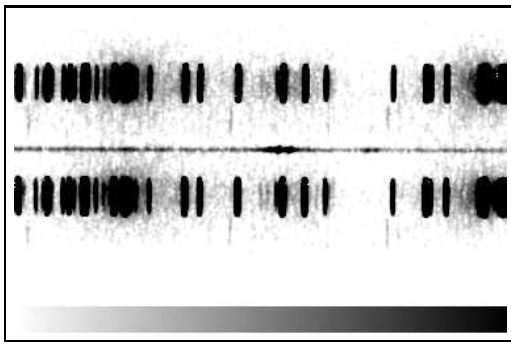


**Fig. 2.** Two-dimensional spectrum of the Seyfert galaxy NGC 7469 taken with the 2.0-m telescope, UAGS and ST-6 CCD camera. The dispersion of the spectrum is 100 Å/mm and the wavelength increases to the right. The region centred on the H $\alpha$  + [NII] 6548/83 emission lines complex and containing the [SII] 6716/31 emission lines doublet is captured. The calibration spectrum of the He-Ne-Ar lamp is visible below and above the object spectrum.

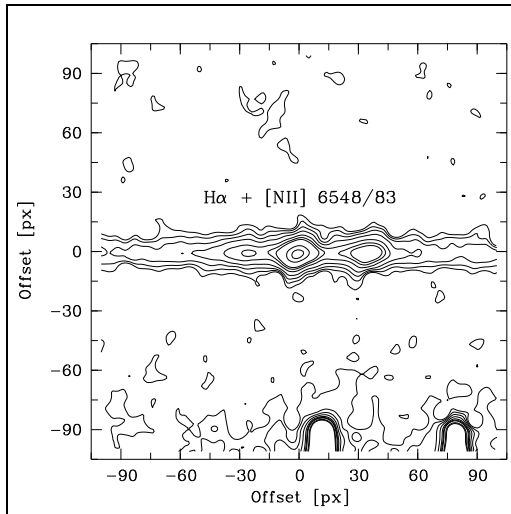


**Fig. 3.** A contour plot of the NGC 7469 spectrum centred on the H $\alpha$  + [NII] 6548/83 emission lines complex. The offset is measured from the H $\alpha$  line peak; the wavelength increase to the right; the pixel size in this contour plot is four times smaller than the original one. The H $\alpha$  and [NII] 6583 line tilting due to the galaxy rotation is clearly visible.

of 2.3 Å/px; the spectral resolution was estimated to be 4 – 5 Å or  $R = \lambda/\Delta\lambda \approx 1500$  at H $\alpha$ . He-Ne-Ar lamp was used for wavelength calibration.

We acquired three exposures of 600 sec duration each; multiple dark current frames of the same exposure time were taken as well. Initial reduction of the frames was done using ESO-MIDAS. The individual dark frames were median combined to a single, super-dark frame to increase the S/N ratio and to clean-up the cosmic ray hits. The object spectra were dark subtracted, cosmic ray hits cleaned, aligned and combined to a single, 1800 sec spectrum that is shown in Fig. 2.

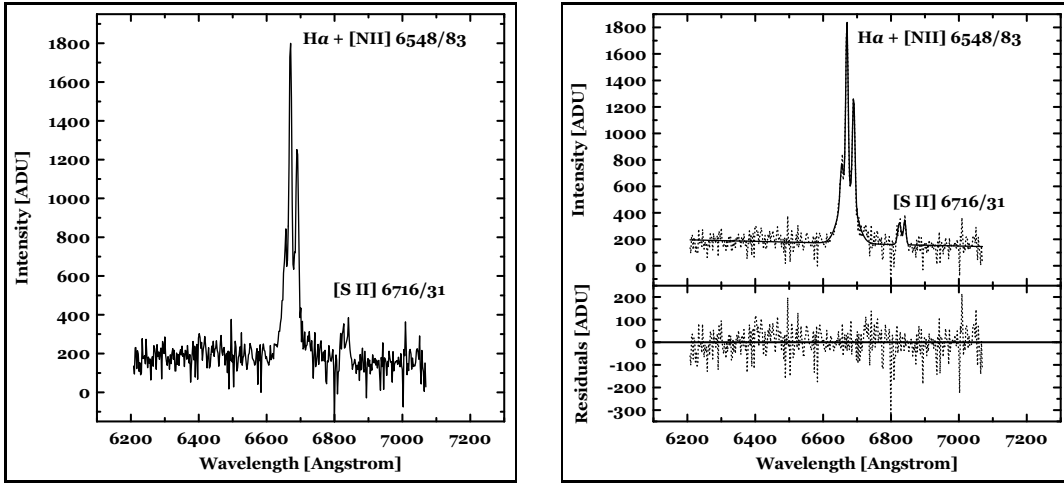


Fig. 4. Left panel: final one-dimensional spectrum of NGC 7469; the spectrum is not flux calibrated. Right panel: overall spectrum fit and fitting residuals.

## 2 One-dimensional spectrum extraction and processing

To obtain the sky spectrum two rows free of object spectrum were extracted – one below and one above the object spectrum – and averaged. We got  $\sigma_{\text{sky}} = 39.1$  ADU. To obtain the object spectrum, a single row was extracted and sky subtracted. We got  $\sigma_{\text{obj}} = 63.2$  ADU; this value was estimated over the whole spectrum, but the region  $6600 - 6860 \text{ \AA}$  where the emission lines are situated (see Fig. 4). A single row was extracted because the emission lines are tilted due to the galaxy rotation as can be seen in Fig. 3. The estimated S/N ratio is about 28 for the  $\text{H}\alpha$  line and about 6 for the [SII] ones.

The wavelength calibration was done using the He-Ne-Ar lines visible below and above the object spectrum (see Fig. 2). We used a total of 15 comparison lines. A linear fit was performed between the wavelength (in Angstroms) and the position (in pixels) and the positions along the dispersion were converted into wavelengths. The accuracy of the wavelength calibration was estimated to be  $\pm 0.45 \text{ \AA}$ ; this is actually the standard deviation<sup>3</sup> about the fitted line. The final one-dimensional spectrum is shown in Fig. 4, left panel; flux calibration was not performed.

## 3 Emission lines decomposition

The spectral region covered by our spectrum was fitted with 6 Gaussians for the emission lines – 4 for the  $\text{H}\alpha + [\text{NII}]$  complex and 2 for the [SII] doublet – plus a first order polynomial for the continuum; the fit was unweighted one and all components were fitted simultaneously. The composite fitting function reads

$$I(\lambda) = a + b\lambda + \sum_i I_i(\lambda_0) \exp \left[ -0.5 \left( \frac{\lambda - \lambda_{0,i}}{\sigma_i} \right)^2 \right],$$

<sup>3</sup> We scaled the sum of the squared residuals by  $N - M$ , where  $N$  is the number of the fitted data points and  $M$  is the number of the fitting parameters; in the case of standard deviation about the mean value one has  $M = 1$ .

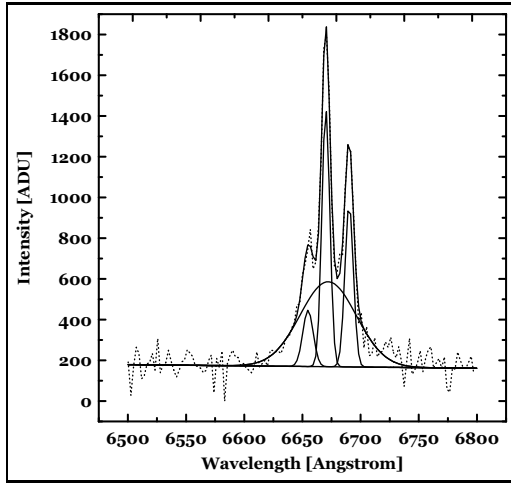


**Fig. 5.**  $H\alpha + [NII] 6548/83$  emission line complex decomposition into 4 Gaussians plus a linear continuum.

**Table 1.** Parameters of the fitted Gaussians.

Component	$\lambda_0$ [ $\text{\AA}$ ]	$I(\lambda_0)$ [ADU]	$\sigma$ [ $\text{\AA}$ ]
[NII] 6548.05	$6654.84 \pm 0.82$	$276.66 \pm 58.08$	$4.46 \pm 1.02$
$H\alpha$ 6562.801 (narrow)	$6670.14 \pm 0.16$	$1269.23 \pm 68.93$	$3.42 \pm 0.22$
$H\alpha$ 6562.801 (broad)	$6672.20 \pm 1.77$	$417.34 \pm 60.37$	$24.11 \pm 1.78$
[NII] 6583.45	$6690.16 \pm 0.26$	$797.53 \pm 53.39$	$3.64 \pm 0.33$
[SII] 6716.44	$6824.91 \pm 1.53$	$163.75 \pm 38.86$	$5.21 \pm 1.68$
[SII] 6730.82	$6840.60 \pm 1.12$	$185.55 \pm 46.24$	$3.49 \pm 1.15$

where  $a$  and  $b$  are the intercept and slope of the continuum, respectively,  $\lambda_0$  is the central wavelength,  $I(\lambda_0)$  is the intensity at  $\lambda_0$ ,  $\sigma$  is the Gaussian sigma and  $i$  counts the Gaussian components included. The resulting fit is overplotted onto the observed spectrum in Fig. 4, right panel, and the fitted model parameters are listed in Table 1; the wavelength calibration error should be added in quadrature to the errors of the central wavelengths listed in Table 1 before their further use. One could see that the chosen composite fitting function represents the overall spectrum fairly well; the standard deviation of the residual spectrum is 61.6 ADU – a value compatible with the spectrum noise. Therefore, no additional noise is introduced by the decomposition. The spectral decomposition of the  $H\alpha + [NII]$  complex is presented in Fig. 5. The  $H\alpha$  line is fitted by two components – a narrow one and a broad one – which is typical for intermediate Seyfert type nuclei. The central wavelengths of the  $H\alpha$  broad and narrow components are the same to within the errors.

The weight-mean redshift determined using the narrow lines plus the narrow  $H\alpha$  component is  $0.01629 \pm 0.00005$ . The weight-mean FWHM of the narrow lines plus the narrow  $H\alpha$  component is  $8.33 \pm 0.42 \text{ \AA}$  ( $7.46 \pm 0.52 \text{ \AA}$ ), whereas the FWHM of the broad  $H\alpha$  component is  $56.78 \pm 4.19 \text{ \AA}$  ( $56.66 \pm 4.20 \text{ \AA}$ ) or  $2593.74 \pm 191.40 \text{ km s}^{-1}$  ( $2588.26 \pm 191.86 \text{ km s}^{-1}$ ); the corresponding values corrected for the finite line width are given in the parenthesis. The correction was done according to the formula:

$$\mathcal{FW}_{\text{corr}}^2 = \mathcal{FW}_{\text{obs}}^2 - \mathcal{FW}_{\text{instr}}^2,$$

where  $\mathcal{FW}_{\text{corr}}$  is the corrected FWHM,  $\mathcal{FW}_{\text{obs}}$  is the observed FWHM and  $\mathcal{FW}_{\text{instr}}$  is the instrumental FWHM (see Sect. 4 for the instrumental FWHM determination).

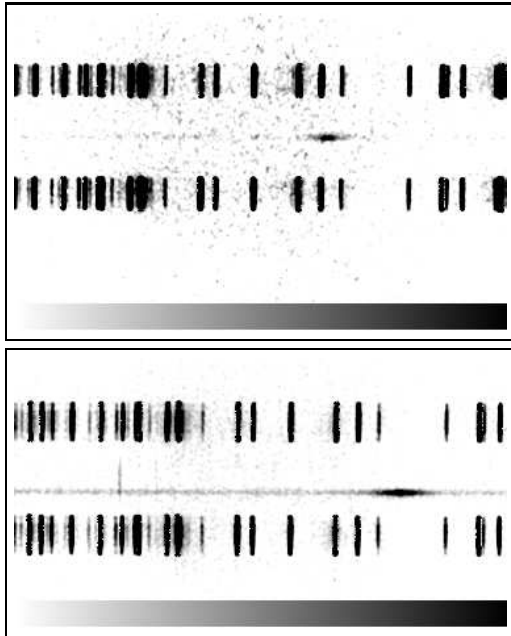


**Fig. 6.** Spectra of the Seyfert galaxies Mrk 335 (upper panel) and Mrk 509 (lower panel) around the  $H\alpha + [NII]$  emission lines complex. Wavelength increases to the right. The night sky emission line  $[OI] 6300$  is visible in the Mrk 509 spectrum.

#### 4 Other Seyfert galaxies observed with UAGS

The Seyfert galaxies Mrk 335 and Mrk 509 were observed during the August/September 2003 UAGS testing run as well; the same observational setup and strategy as in NGC 7469 observations were used. However, the spectra we obtained were of lower quality – the estimated S/N ratio for the  $H\alpha$  line was about 6 for Mrk 335 and about 13 for Mrk 509. The individual spectra were dark subtracted, cosmic ray hits cleaned, aligned and combined. The one-dimensional spectrum was obtained by summing – along the columns – the rows occupied by the object spectrum. The same number of rows – not contaminated by the object spectrum – were summed to obtain the sky spectrum. The spectra of Mrk 335 and Mrk 509 are shown in Fig. 6 and Fig. 7. Due to the low S/N ratio and the complex structure of the  $H\alpha$  region the emission lines decomposition was not performed.

In the original spectrum of Mrk 509 the night sky emission lines  $[OI] 6300/64$  are visible; in Fig. 6 only  $[OI] 6300$  could be identified. These lines were used to estimate the instrumental line width. For this purpose the one-dimensional sky spectrum was wavelength calibrated and the region containing the  $[OI]$  lines was fitted with 2 Gaussians plus a linear continuum in the same way as for NGC 7469. The central wavelengths we got are  $6299.44 \pm 0.26 \text{ \AA}$  and  $6363.14 \pm 0.60 \text{ \AA}$ ; the laboratory values are  $6300.304 \text{ \AA}$  and  $6363.780 \text{ \AA}$ . The weight-mean FWHM of the  $[OI]$  lines is  $3.71 \pm 0.44 \text{ \AA}$  and it was used to correct the FWHM of the observed emission lines for the instrumental line width (see Sect. 3).

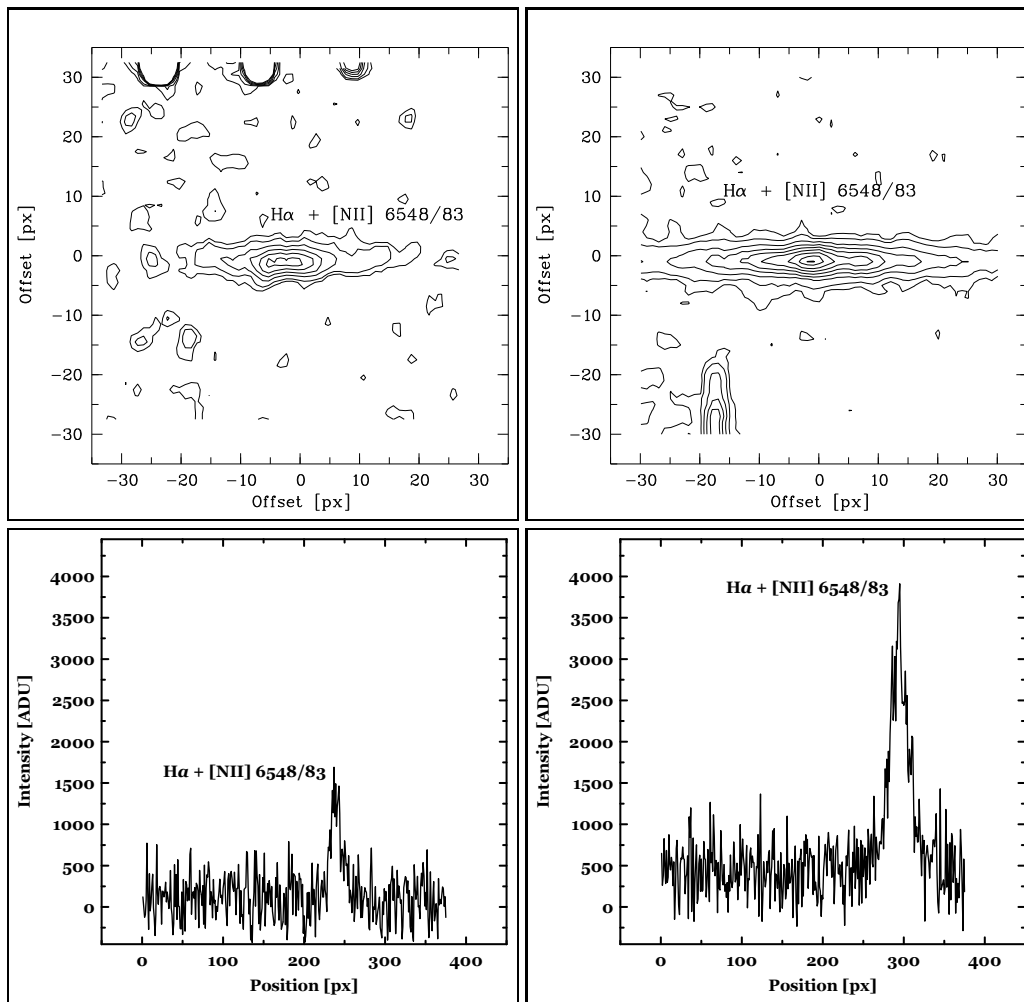


**Fig. 7.** Two- (upper panels) and one-dimensional (lower panels) spectra of Mrk 335 (left panels) and Mrk 509 (right panels) around the H $\alpha$  + [NII] emission lines complex. Offset is measured from the H $\alpha$  peak in upper panels. Wavelength increases to the right.

## Conclusion

Our study showed that UAGS could successfully fill the gap between the high resolution spectroscopy with the Coudé spectrograph and the low resolution spectroscopy with FoReRo/FoReRo-2 and to become a useful part of the spectral apparatus at NAO.

## Acknowledgments

The design and manufacturing of the Focal Reducer Rozhen (FoReRo) were performed in the workshop of the Institute of Astronomy, Bulgarian Academy of Sciences, with financial support by the Ministry of Education and Science, Bulgaria (contract F-482/2201).

## References

- Semkov E., Bachev R., Strigachev, A., 2005, *Aerospace Research in Bulgaria*, 20, 99  
Slavcheva L., Petrov G., Mihov B., 1998, *Comptes rendus de l'Académie bulgare des Sciences*, 51, 5  
Tsvetkov M. K., Markov H. S., 1984, *Comptes rendus de l'Académie bulgare des Sciences*, 37, 11